ISSN: 0067-2904

Assessment of Environmental Pollution using Electrical Resistivity and Logging Techniques over A Municipal Dumpsite of Ijagun Ijebu Ode

N. O. Adebisi[1], O.O. Bayewu*[1], S.O. Ariyo,[1] G.O. Mosuro[1], O. M. Oloruntola[2], A.O. Alaka,[1] and O. O. Odugbesan[1]

[1]*Department of Earth Sciences, Olabisi Onabanjo University, Ago Iwoye, Nigeria*
[2]*Department of Geosciences, University of Lagos, Lagos, Nigeria*

Received: 27/8/2020 Accepted: 21/6/2021

Abstract

The present study aims to assess environmental pollution using theresistivity method and geological logging technique over a municipal dumpsite of Ijagun Ijebu Ode, underlain by theAfowo Formation within the Dahomey Basin southwestern Nigeria. Forty vertical electrical resistivity soundings stations and six 2D electrical resistivity imaging profiles using Schlumberger and Wenner array respectively with maximum spread-length of 40m at each sounding and profile length of 60 m and 120 m and one borehole log were carried out. Three geoelectrical layers were obtained in the control area, their resistivity values with their corresponding depth of sediment materials is 126 Ωm – 724 Ωm at depth range 0.9 m – 1.1 m (topsoil), 608 Ωm – 2517 Ωm at depth range 3.5 m – 17.7 m (sandy layer), and 800 Ωm – 6046 Ωm (dry sandy layer). Along with the 2D resistivity imaging profiles over the control (1 and 2), four geo-electric layers characterized by Resistivity values range of 40 Ωm – 126 Ωm (loam), 135 Ωm – 418 Ωm (loamy sand), 500 Ωm – 1500 Ωm (sandy), and >3000 Ωm (dry sand) were revealed. The lithology recovery from the logging techniques shows the subsurface is underlined chiefly with sand, which shows a significant correlation with the geophysical method. The lower values of resistivity at the dumpsite are clear evidence of the subsurface contamination of the sandy layer. The 2D images revealed the contaminated zone thickness ranges from 2 m in the northwest to 25 m in the southeastern part. The protective capacity map derived from the VES showed that the dumpsite is underlain by poorly protected sandy lithology, prone to leachate infiltration. Relocation of the dumpsite to a better protected environment or underlining the present area with an impermeable geotextile layer would halt further leachate invasion into the subsurface.

Keywords: Dumpsite, Contamination, Leachate, Vertical Electrical Sounding, Electrical Resistivity Imaging.

Introduction

The influence of anthropogenic contamination on the environment is continuously affecting the subsurface as the volume of waste generation increases due to increase in population, urbanization, and industrialization; more devastatingly through the assigned localized dumpsites for such purposes. Waste generation is inevitable in virtually all ramifications of man's productive accomplishments [1]. The enormity of health problems originating from environmental hazards associated with waste generation is relatively prevalent in developing countries like Nigeria due to improper management [2-3]. Poor coordination of the open-pit

*Email: bayewu.olateju@oouagoiwoye.edu.ng

dumping system practised in Nigeria raises serious concern about leachate formation and infiltration mechanisms. Under the tropical humid condition, heavy rainfall over the dumps accelerates waste liquefaction and aids the ionization of inorganic compounds to form a solution of highly conductive mobile salty substrates [4-5] and organic matter, which permeates through the zone of aeration, and may practically invade the groundwater resources within the saturation zone [6]. Leachate mobility rate from dumpsite into the subsurface is greatly influenced by several geological factors, including the porosity and permeability attributes of underlying lithologic assemblage, favourable absence or inimical presence of secondary structures, depth to the water table or piezometric surface, and the prevailing geothermal gradient [7].

The suitability of the electrical resistivity method as an aid for contamination plume mapping has been extensively proven in the different published works of several authors [8-18]. However, the approach of lithological logging has also been used in the context of some research work [1], [14], and it. It has been found successful because it allows the physical observation of the surface lithologic layer rather than inferring from the remote method. The only disadvantage of this method is that it gives information only about the point of drilling and neglects lateral variation in lithology. It is, is also very costly to carry out. The present study also involves the electrical resistivity method using geoelectric parameters and lithologic logging method to map the near-surface geological materials overlying the aquifer against contaminants and its tendency to restrict contaminants infiltration. The aim of this research is to study the environmental pollution impacts of the dumpsite in the study area through an electrical resistivity survey and lithological information within the area.

Location and Geology of the Study Area

The study area (Figure 1) covers Ijagun dumpsite and its adjacent areas along Ore – Benin Expressway, Southwestern Nigeria, which is located between latitude and longitude within 6.789258˚N to 6.793383˚N and 3.937124˚E to 3.942557˚E respectively in a decimal format of the coordinate system unit. The area is directly accessible through the highway and other path linkages leading to the area. There is poor accessibility to the depressed southern part because of its swampy nature.

The area falls within the Dahomey Basin and geologically belongs to the Abeokuta Formation, which is divided into three recognizable formations: Ise Formation (Albian), Afowo Formation (Turonian) and Araromi Formation (Maastrichtian), and they are overlying one another. These formations are seated uncomformably on the Precambrian Basement rock. The whole of the study area predominantly lies on the Ise Formation, which is the basal part of the three formations comprised of conglomerates and sands, which conform with the lithological log of drill well in the study area. The succession continues upwards with medium to coarse, loose sands interbedded with Kaolinitic clays. The basin is a southerly warping arcuate structural depression (Figure 2) sympathetically originated in response to the regional transcurrent stresses associated with the divergent detachment of African and South American plates from each other [19]. The rifting event in the Late Jurassic to Early Cretaceous opened up large accommodation space for the deposition sediments of diachronous ages [20] (Figure 3). The geographical dimension of the basin stretches regionally across four West African countries; southeastern Ghana, Togo, Benin and the sedimentary portion of southwestern Nigeria, terminating along the Benin hinge line [21]. Based on chronological succession, the stratigraphy of the basin was deposited during three major eras [22]; the Late Cretaceous continental sequence, known as the Abeokuta group, the Tertiary sequence comprising thick basal marine sediment interrupted by several regressive events and the Quaternary coastal sediments. The average elevation of the study location from sea level ranges between 187-208m. The hydrogeology of the Ijagun area reveals the main aquiferous layer in the study area is the sand layer which is mostly medium-coarse in texture. The aquiferous layer in the study

area occurs with an average depth range of 22m-45m. Before encountering the aquiferous layer, overburden in the study area includesincludes the unconsolidated sand layer, which occurs mainly as topsoil, lateritc soil which is mainly above the dry sand layer.

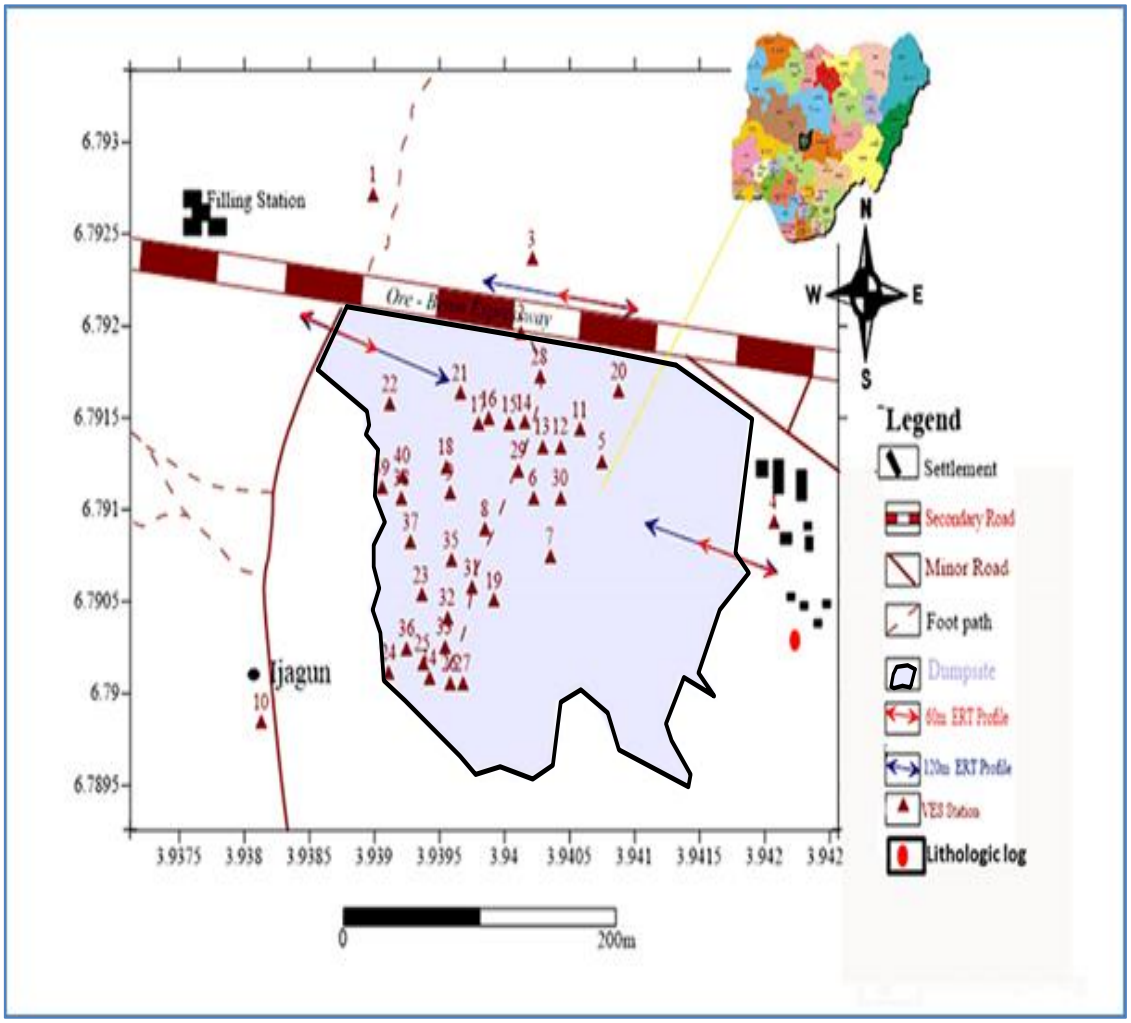

Figure 1- Location Map of the Study Area showing the VES locations, the 2D profiles and the lithologic log.

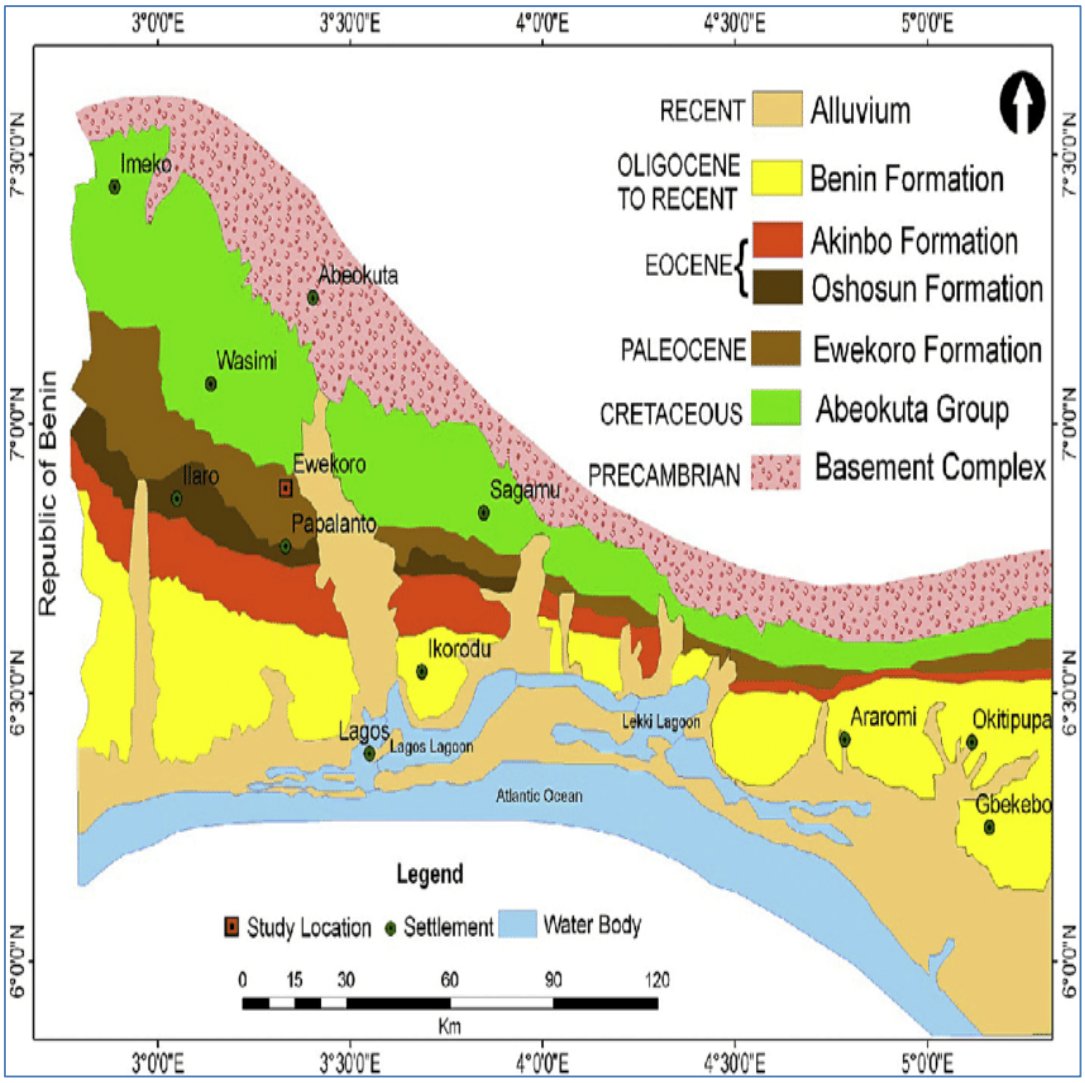

Figure 2-Geological map of the eastern Dahomey Basin (Nigerian part) and location of sample collection-Ewekoro Quarry [23].

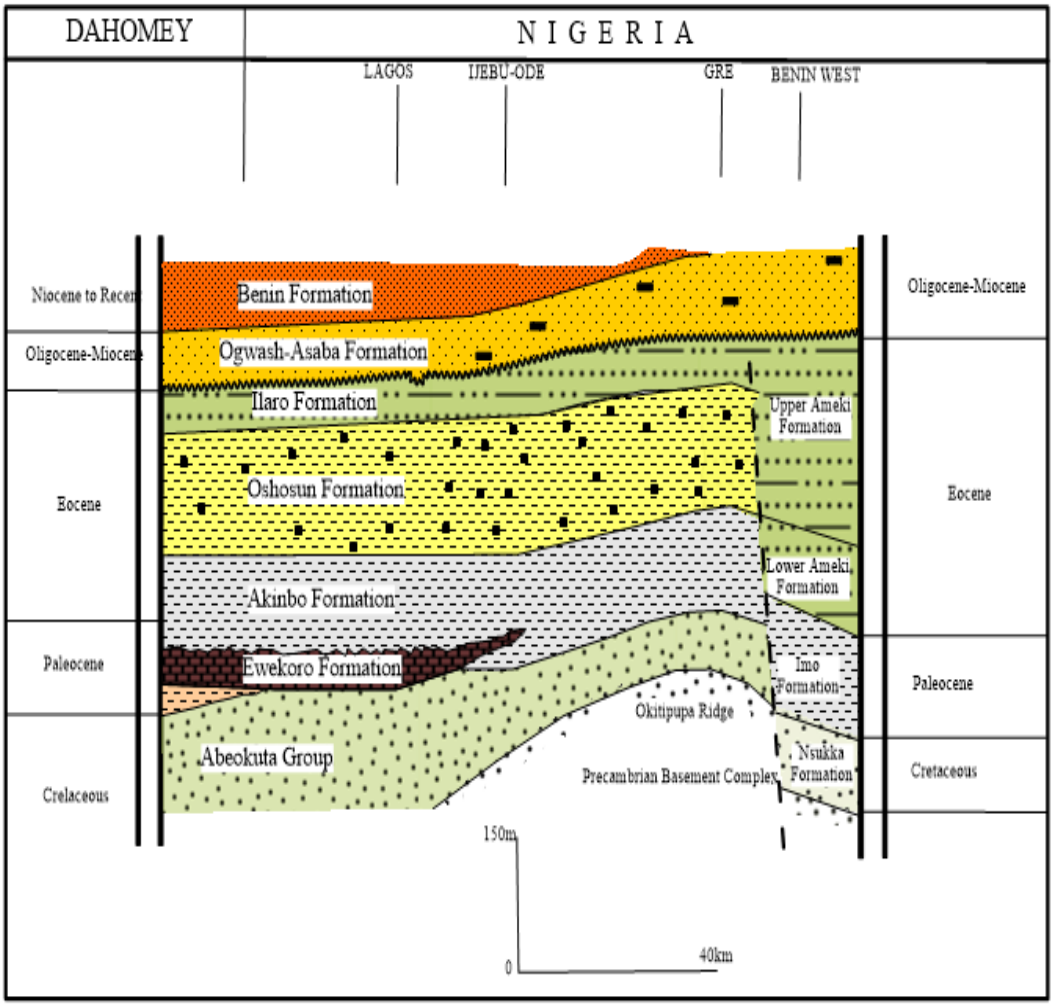

Figure 3- The stratigraphic column of Eastern Dahomey Basin (after [24]).

Methods and Materials

Electrical Resistivity Method

Vertical electrical sounding (VES) and 2D electric resistivity imaging (ERI) techniques were used to determine the extension and shape of the dumpsite into the underlying sedimentary formation. The Schlumberger array was used to acquire forty (40) VES pointspoints while the Wenner arrays electrode configuration was used to establish six (6) profiles in the area. Field procedure for four electrodes sounding survey involves station establishment, circuitry connection to the earth, current transmission into the subsurface via the current electrodes, potential difference measurement by the inner potential electrode pair, resistance calculation in accordance to Ohm's law and automated apparent resistivity computation by the adopted SAS 1000 resistivity meter using the appropriate geometrical factors of the selected array. Survey advances with repetition of procedure at ,more significant current electrode separation increment halted by occasional potential expansion to avoid a drastic drop in the measured voltage. The maximum electrode spread length was 40 m (Table 1). With the aid of bi-logarithmic paper, plots of apparent resistivity values against electrode separation revealed the resistivity curve of the investigated spot. Comparison of the apparent resistivity curve with the master curve using the partial matching techniques generated tentative layering parameters (i.e. resistivity value, thickness and depth) adopted as starting model for the iteration process from which the true layering parameters were computed automatic modelling. For the Vertical electrical sounding data obtained, the Protective capacity of the geo-electric strata was

evaluatedusing th longitudinl conductance value, as described by [25-8] (Table 2) was calculated as follows:

$$S = \Sigma\,(hi/\rho i) = h1/\rho 1 + h2/\rho 2 + \ldots + hn/\rho n$$

*Where **S** is the total longitudinal conductance, **hi** is the thickness of the ith Layer, and **ρi** is the resistivity of the ith layer*

A longitudinal conductance value below 0.10 is classified a poor filter, 0.1 – 0.19 as weak, 0.2 – 0.69 as moderate, and 0.7 – 1.0 as a good protector after [22, 3, 24 and15] (Table 3).

Table 1-Obtained resistivity value (Ωm)

AB/2	VES 1	VES 2	VES 3	VES 4	VES 5	VES 6	VES 7	VES 8	VES 9	VES 10
1	568.89	145.88	625.06	290.42	28.74	15.18	35.63	98.58	126.49	816.73
2	666.34	216.35	778.63	251.39	32.07	18.44	40.50	126.65	151.90	1066.84
3	773.37	292.76	894.31	201.84	29.35	21.15	43.19	143.04	184.55	1290.05
4	865.20	388.06	983.68	167.69	30.66	23.62	47.28	158.55	224.84	1494.71
6	1106.40	484.82	1158.87	183.32	29.64	30.12	57.34	188.27	283.42	1921.91
9	1313.71	542.16	1489.79	274.27	33.90	37.35	76.31	213.19	320.57	2340.75
12	1425.41	612.36	1750.96	333.24	47.47	48.68	92.89	215.37	315.76	2433.83
15	1428.42	687.29	1895.35	380.78	57.85	61.42	105.23	200.67	286.87	2381.31
20	1592.14	755.86	2063.40	460.00	65.40	75.24	129.78	204.35	290.49	2367.56
25	1736.56	865.94	2215.67	569.92	76.96	84.72	156.93	224.35	310.10	2501.58
32	1890.48	980.27	2370.45	680.26	104.01	91.21	197.13	261.06	332.05	2980.24
40	2006.03	1183.20	2564.58	757.76	129.75	104.36	217.81	283.03	367.70	3551.06

AB/2	VES 11	VES 12	VES 13	VES 14	VES 15	VES 16	VES 17	VES 18	VES 19	VES 20
1	24.06	46.84	13.80	20.33	46.48	8.60	80.95	29.10	41.84	286.26
2	17.54	49.79	11.64	22.49	32.55	11.36	102.51	24.07	36.00	343.36
3	17.45	56.23	12.90	25.38	25.81	13.98	142.71	21.43	29.28	379.96
4	18.41	67.78	14.92	30.29	22.04	17.38	175.33	20.89	25.42	420.11
6	21.89	74.94	20.80	41.15	21.59	22.49	215.09	25.26	23.50	479.37
9	27.64	81.19	28.72	52.10	27.12	31.41	258.79	32.51	25.86	500.74
12	37.05	85.45	40.33	62.35	32.20	40.81	250.52	36.94	27.87	520.49
15	48.26	93.13	48.31	71.14	41.33	45.74	263.09	44.89	30.11	540.40
20	65.38	106.82	53.16	85.63	55.10	60.79	312.79	57.26	38.97	570.00
25	81.06	118.56	68.51	100.68	69.69	70.04	349.00	66.10	47.28	570.73
32	97.71	133.71	84.43	120.84	96.69	91.99	389.18	80.34	57.21	600.04
40	110.80	157.99	95.23	140.88	122.67	120.23	415.12	95.69	69.53	670.70

AB/2	VES 21	VES 22	VES 23	VES 24	VES 25	VES 26	VES 27	VES 28	VES 29	VES 30
1	47.55	72.28	55.96	12.27	65.06	42.15	38.15	132.49	38.15	51.64
2	70.54	109.24	60.44	10.55	70.77	48.72	59.80	122.69	59.80	71.84
3	98.14	140.56	84.67	10.68	72.79	50.77	75.17	93.69	75.17	84.94
4	121.58	162.14	98.37	12.24	74.09	51.62	92.01	74.02	92.01	101.57
6	151.19	185.53	126.03	16.41	77.38	54.00	106.44	71.54	106.44	142.23
9	199.14	210.80	163.17	23.90	89.69	54.21	128.71	98.60	128.71	162.23
12	219.53	207.71	199.09	30.89	98.58	58.34	129.01	126.84	129.01	169.12
15	203.75	178.25	247.86	35.94	105.25	59.82	125.56	152.75	125.56	161.76

20	189.51	201.32	274.73	42.67	119.00	62.63	138.00	174.36	138.00	169.06
25	186.21	223.77	288.24	50.79	133.40	65.81	160.50	191.83	160.50	173.90
32	190.99	244.02	294.99	59.99	143.03	68.02	189.63	216.21	189.63	194.99
40	201.98	261.85	300.59	69.89	162.97	72.21	231.51	225.24	231.51	230.51

AB/2	VES 31	VES 32	VES 33	VES 34	VES 35	VES 36	VES 37	VES 38	VES 39	VES 40
1	62.00	154.67	92.97	43.70	233.89	106.70	58.15	95.88	85.64	34.10
2	79.97	168.67	136.25	47.04	259.25	98.04	68.72	126.35	108.84	50.07
3	91.26	185.80	165.81	52.61	294.87	88.61	76.77	162.76	130.94	62.43
4	98.91	203.59	188.48	58.20	325.62	83.20	78.62	208.06	140.57	75.89
6	103.27	234.61	229.96	68.14	385.77	85.21	84.00	24.82	170.00	92.26
9	110.70	271.76	273.37	72.86	456.39	87.86	90.21	312.16	205.00	106.51
12	116.97	307.33	300.19	80.45	503.51	98.45	103.34	352.36	230.00	118.94
15	123.59	350.47	312.43	83.02	536.77	102.02	111.23	397.29	280.76	131.18
20	129.67	397.93	337.68	90.42	584.53	115.42	123.63	445.86	298.06	155.26
25	133.01	423.98	358.55	98.40	654.17	120.40	135.13	535.94	315.90	170.10
32	140.33	431.59	391.75	109.17	694.53	130.17	151.02	600.27	362.00	185.34
40	144.19	458.14	417.12	124.10	724.59	141.10	162.21	703.20	375.00	201.69

Table 2-Protective Capacity Classification Scheme of Earth Materials [15, 16 and 27]

Total longitudinal Conductance (Ω-1)	**Protective capacity classification**
<0.10	Poor
0.1 – 0.19	Weak
0.2 – 0.69	Moderate
0.7 – 1.0	Good

The basic procedure for acquiring ERI data with the aid of the Wenner array involved the sequential advancement of equally spaced electrodes from the starting position along with the profile until the last possible measurement was made. Repeated measureswere then made at multiple separation intervals using the same procedure for up to five levels were (i.e. n=5). Six resistivity profiles were imaged along with three selected survey locations such that at each location, two distinct resistivity imaging surveys were separately conducted along a profile length of 60 m using a constant electrode spacing interval (a) of 2 m and along an extended spread length of 120 m using electrode spacing interval (a) of 5 m – both maintaining same starting position. The profile of a= 2 m with 60 m spread high-resolution imaging surveys designed to simulate waste encroachment into the adjoining areas. In comparison,the profile of a= 5 m with 120 m spread provided an intensive mapping of differential spatial concentration and the infiltration depth within the invaded lithologies. To establish a proof of contamination, a control survey location was essentially positioned about 40 m away from the dump whilst the other two locations sites are largely situated within the dumpsite with slight extension into the adjoining area (Figure 1). The plot of pseudo sectionpseudo section presentation of apparent resistivity and depth of probing data marked the commencement of the data processing stage. Through the resistivity inversion process using the DIPRO program, the true resistivity of the subsurface was determined for geologic modelling and interpretation.

Lithological Coring Method

The coring was established for one borehole well to determine the geology of the study location using a continuous Shell and Auger which mechanically excavates and transport the cuttings with varying sizes of 4 to 12 inches in diameter for better recovery because of little or no water requirement during the drilling process.

Results and Interpretation

Vertical Electrical Sounding (VES) Results

Layering parameters of the entire resistivity waveforms at the various acquisition stations are presented in table 2. Three geoelectric layers were consistently uncovered at all the VES stations, perhaps due to the electrode separation (AB = 40 m) adopted for the research. A comparative study of these parameters in the study area explicitly revealed a remarkable disparity in resistivity properties over the dumpsite and the bounding vicinity from the interpretation process of the obtained values from the partial curve matching and computerized iteration programs. The iterated curve representation of four vertical electrical sounding points is shown in figure 4.

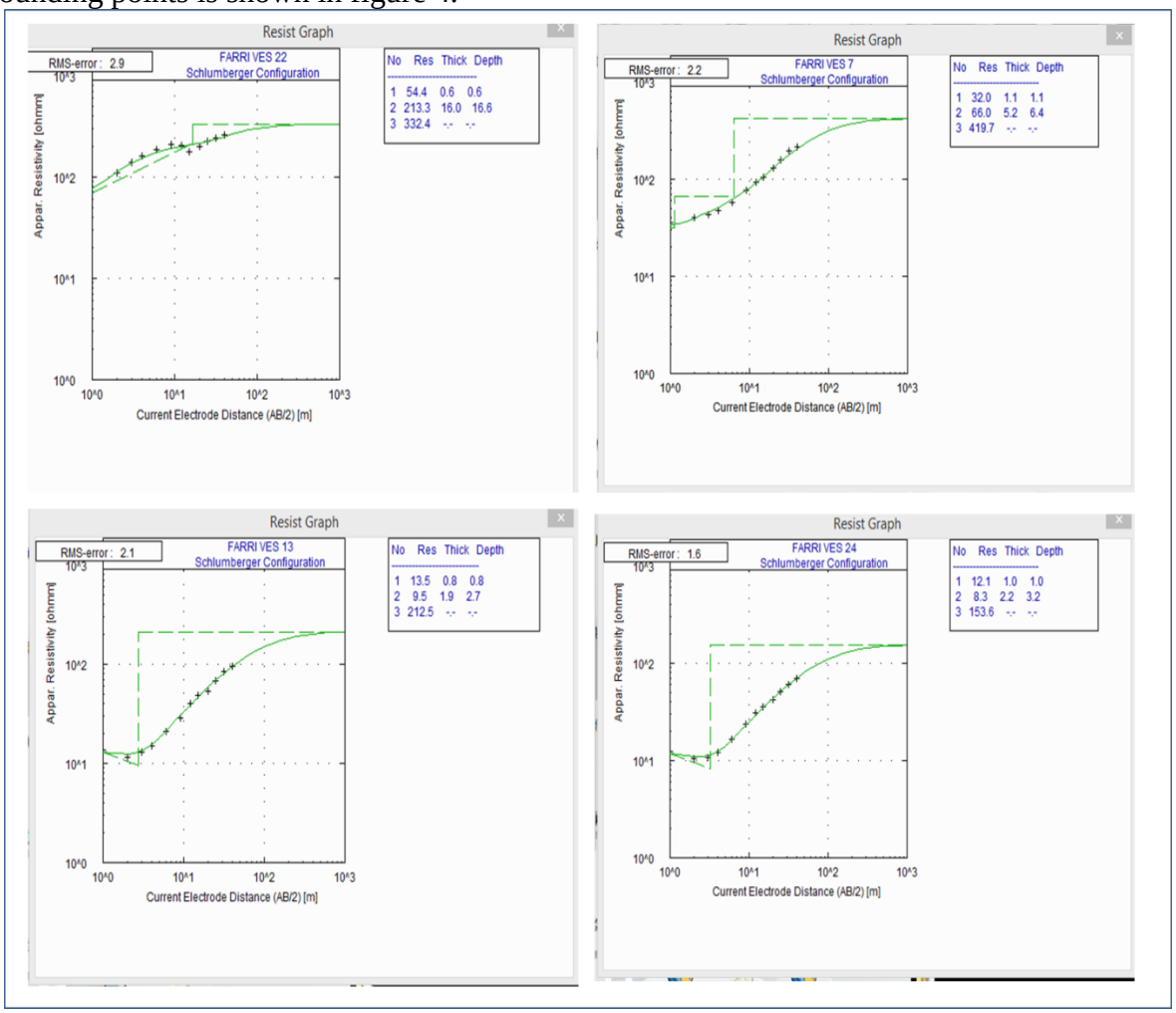

Figure 4- The iterated curve of established vertical electrical sounding point in the study location.

Table 3-Calculated Geo-electric Parameters of Ijagun Dumpsite

VES	ρ1(Ωm)	d(m)	L.I	ρ2(Ωm)	d2(m)	L.I	ρ3(Ωm)	L.I	L.C	C.T
1	529	1.1	T	1210	4.6	S	2295	DS	0.0048	A
2	126	0.9	T	732	6.8	S	1398	S	0.0151	A
3	593	1	T	1372	6.6	S	3551	DS	0.0057	A
4	339	0.9	T	124	4.1	CS	1204	S	0.0027	H
5	31	1.3	RLT	26	6.4	SCS	373	CS	0.2418	H
6	14	1.1	RLT	33	4.7	SCS	159	CS	0.1884	A
7	32	1.1	RLT	66	6.4	SCS	420	CS	0.11315	A
8	87	0.7	RLT	199	19.3	CS	800	S	0.1012	A
9	111	0.9	T	325	41.3	CS	1519	S	0.1324	A
10	724	1	T	2517	18.7	S	6046	DS	0.0084	A
11	24	0.8	RLT	15	4.4	SCS	442	CS	0.2803	H
12	43	1.1	RLT	79	6.4	SCS	175	CS	0.0929	A
13	14	0.8	RLT	10	2.7	SCS	213	CS	0.2592	H
14	19	1.1	RLT	32	4.4	SCS	283	CS	0.1597	A
15	50	1	RLT	15	5.4	SCS	625	S	0.3214	H
16	7.8	1.1	RLT	32	6.5	SCS	545	S	0.3107	A
17	74	1	RLT	297	15.3	CS	999	S	0.0616	A
18	30	1	RLT	16	4.3	SCS	149	CS	0.2399	H
19	44	1	RLT	22	10.7	SCS	196	CS	0.4559	H
20	353	1	T	608	5.2	S	262	CS	0.00973	K
21	36	0.8	RLT	273	11.3	CS	144	CS	0.0606	K
22	54	0.6	RLT	213	16.6	CS	332	CS	0.086	A
23	52	1.6	RLT	342	31.5	CS	1052	S	0.1254	A
24	12	1	RLT	8	3.2	SCS	154	CS	0.3477	H
25	64	1	RLT	82	9.5	SCS	281	CS	0.1193	A
26	44	1	RLT	53	13.5	SCS	125	CS	0.2563	A
27	54	0.9	RLT	147	11.2	CS	347	CS	0.0875	A
28	149	1.2	RLT	48	4.3	SCS	360	CS	0.0072	H
29	35	0.8	RLT	143	22.1	CS	1698	S	0.1716	A
30	44	0.9	RLT	186	32.4	CS	1085	S	0.19008	A
31	62.3	0.9	RLT	116	19.9	CS	381	CS	0.1788	A
32	140	1.1	T	282	9.8	CS	766	S	0.0383	A
33	89	1	RLT	318	13.1	CS	734	S	0.0493	A
34	41	1.1	RLT	72	5.9	SCS	138	CS	0.0947	A
35	210	1.1	T	472	11.3	CS	1138	S	0.0268	A
36	108	1	T	74	5.1	SCS	160	CS	0.065	H
37	29	1.3	RLT	77	15.7	SCS	565	S	0.2321	A
38	95	1.4	RLT	448	6.1	CS	830	S	0.0148	A
39	79	1.1	RLT	224	5.3	CS	462	CS	0.0326	A
40	39	1.2	RLT	109	3.5	SCS	219	CS	0.0529	A

Higher resistivity values ranging 126 Ωm – 724 Ωm, 608 Ωm – 2517 Ωm, 800 Ωm – 6046 Ωm were recorded from top to base of the delineated subsurface section (Figure 5) at control stations: which are interpreted as topsoil, sand and dry sand for the first, second and third geo-electric unit respectively; all of which are sand facies exhibiting increasing resistivity with depth. The depth range of the first and second geoelectric layers is 0.9 m – 1.1 m and 3.5 m – 17.7 m (Figure 5). Resistivity attributes of strata segment underlying the dumpsite dropped anomalously across the entire mapped sections (Figures 6, 7 and 8); resistivity values range between 7.8 Ωm – 149 Ωm and 0.6 m – 1.6 m depth for the topmost stratum, 15 Ωm – 342 Ωm and 1.9 m – 40.4 m depth for the succeeding (second) stratum, and 125 Ωm – 462 Ωm for the basal (third) layer. The low values of resistivity showed evidence of the effect of the dumps on this area, and logically the corresponding inferences for the observed layering pattern are as follows in the previous order; refuse laden topsoil, severely contaminated sand and contaminated sand.

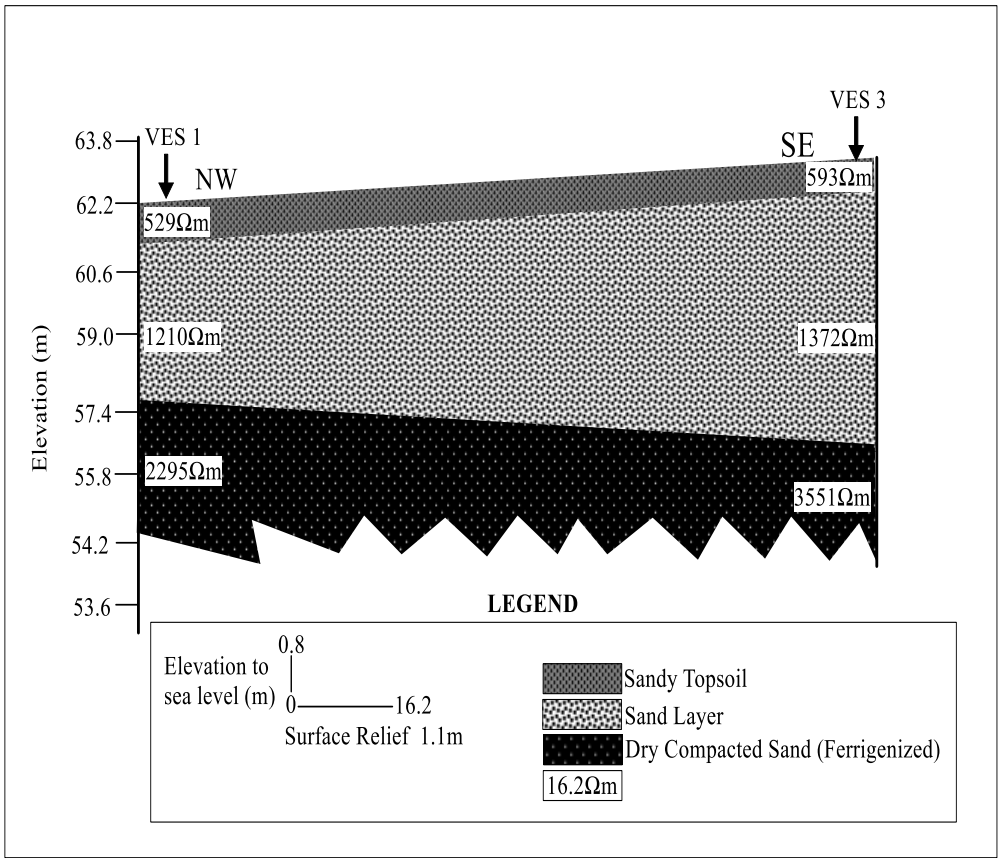

Figure 5- Geoelectrical section which corresponds with the geological section along Traverse 1

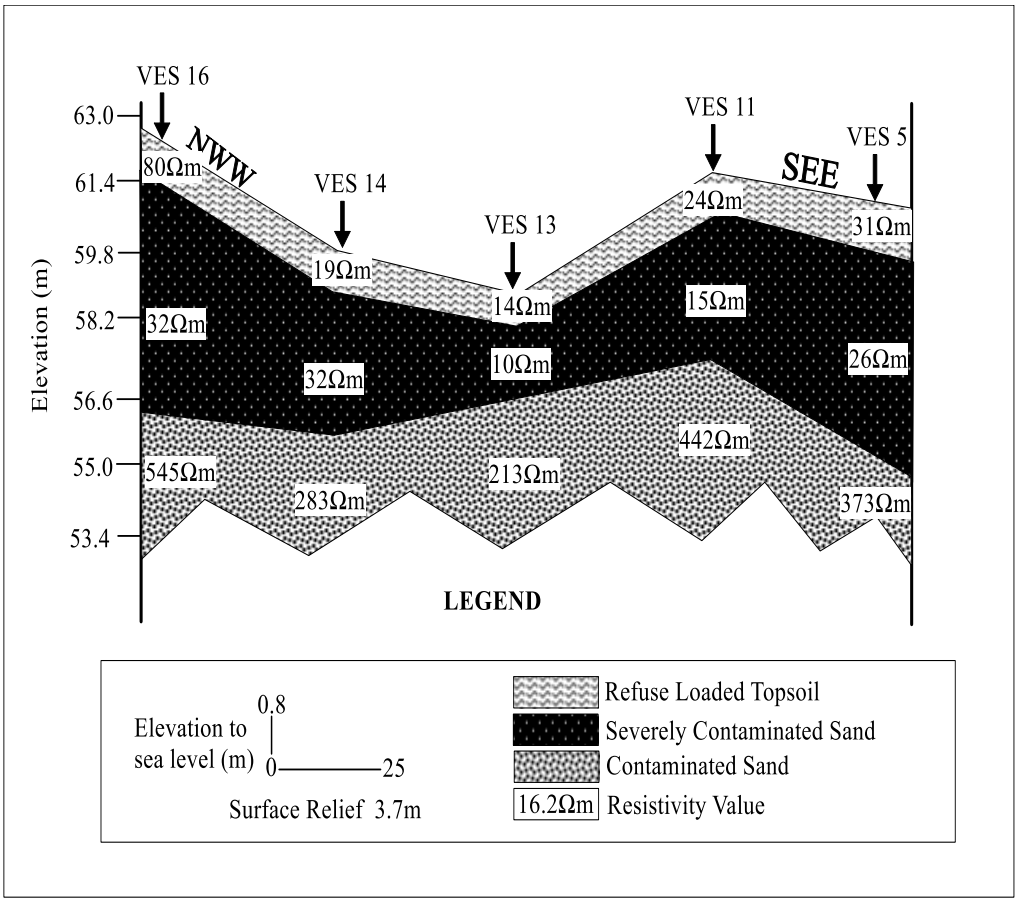

Figure 6-Geoelectrical section which corresponds with the geological section along Traverse 2

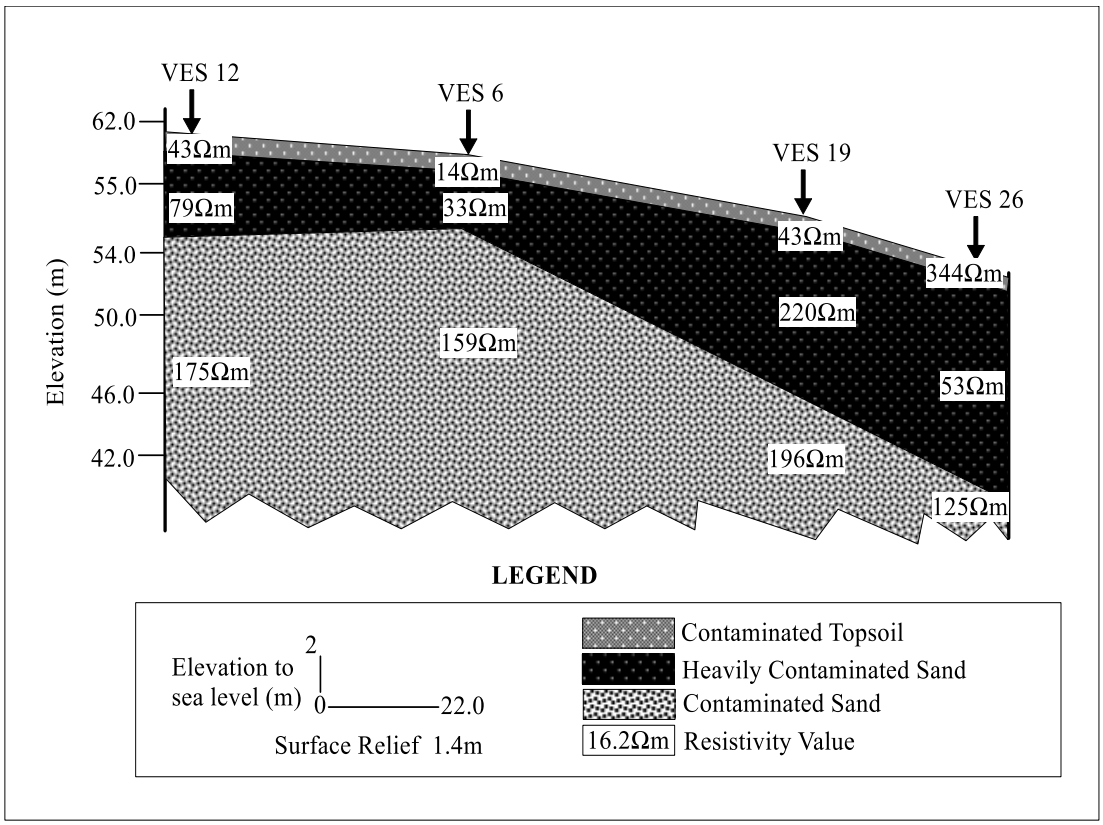

Figure 7- Geoelectrical section which corresponds with the geological section along Traverse 3.

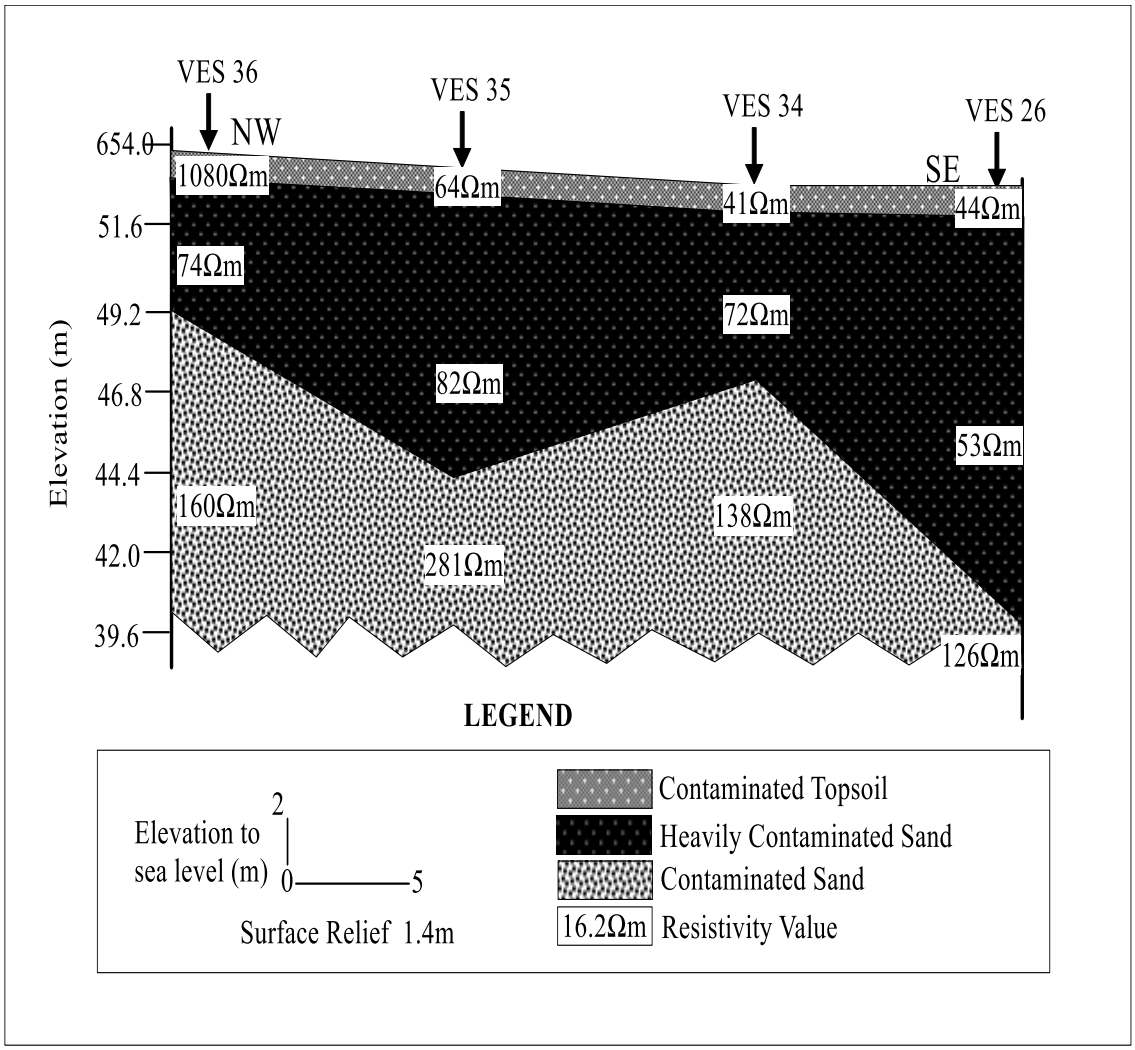

Figure 8-Geoelectrical section which corresponds with the geological section along Traverse 4.

The stacking of the plot of the apparent resistivity map of the dumpsite at different current electrode spacing (AB/2) of 1 m, 6 m, 12 m and 20 m is shown in Figure 9. This plot excluded the control area to have clear information about the leachate infiltration as the depth of probe increases. In qualitative terms, the severity of contamination is noticeably uneven due to variation in concentration level, physical state and salinity content. The leachates in the infiltrated sediments of the dumpsite generally showed a decrease with depth. This agreed with the iterated resistivity data as it increases with depth (Figure 9), thereby increasing the volume of the clean sand the depth increases. Hence, a direct relationship can be established between the conductivity of a formation and the degree of contamination of the sand formation in this area (Figure 9).

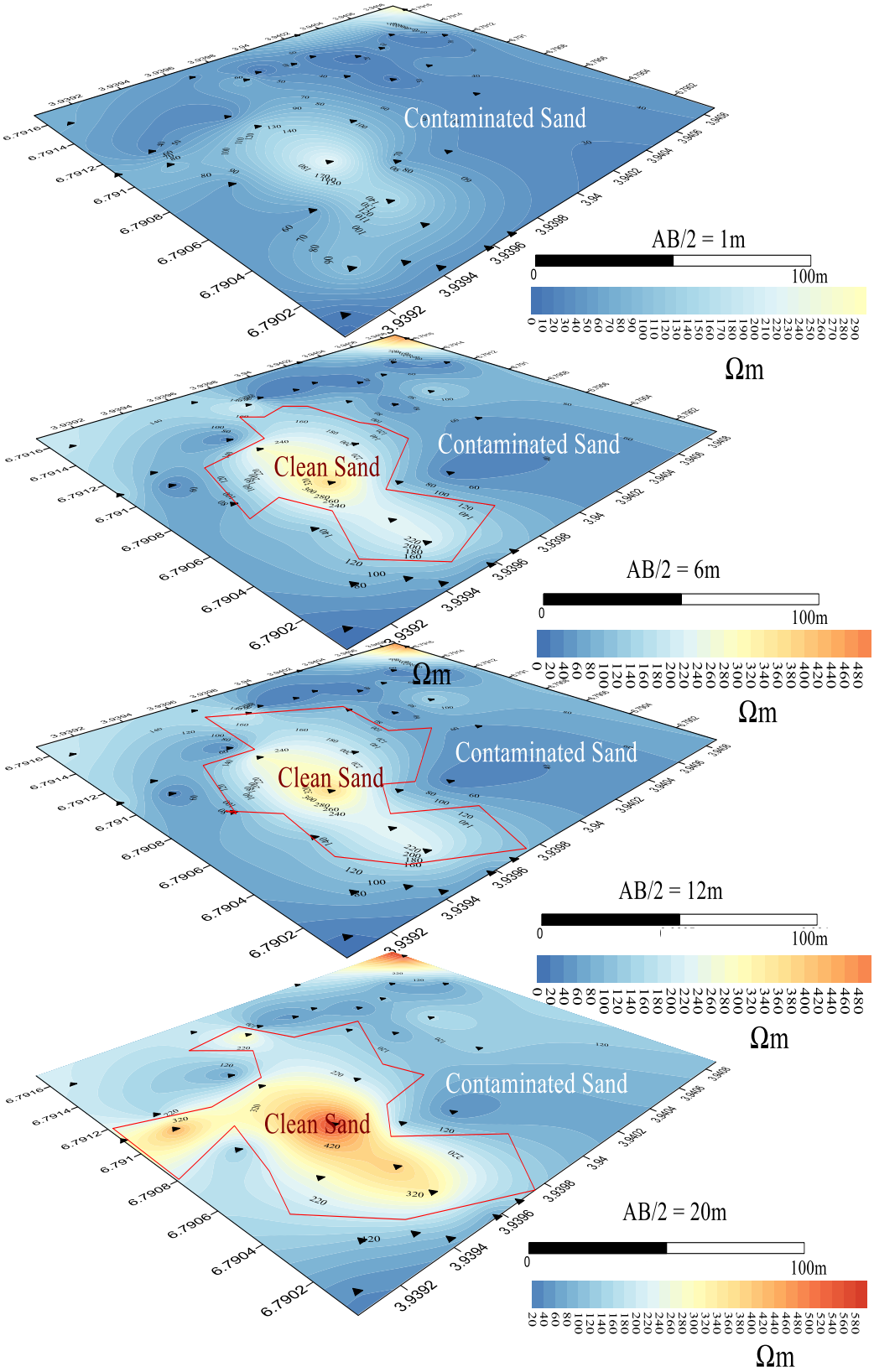

Figure 9- Stacked Isoresistivity Maps of the Ijagun Dumpsite. VES stations at control area excluded.

Electrical Resistivity Imaging Results

The 2-D resistivity imaging models of the six electrical resistivity imaging profiles acquired in the area are presented in Figures 10 to 15.

Control Location (Profiles 1 and 2)

The first profile delineated four geo-electric layers of contrasting resistivity and thickness values (Figure 10). The blue marked uppermost layer denotes a resistivity values and thickness range of 40 Ωm – 120 Ωm and 0.5 m – 1.1 m respectively, thinning out around the southeastern part of the study area. The green coded zone directly beneath is a relatively better resistive and thicker geo-electric stratum with a corresponding value range of 135 Ωm – 418 Ωm and 1.0 m – 3.5 m. Next down the succession is a lemon-yellow geoelectric layer, characterized by a further increase in resistivity magnitude, ranging between 601 Ωm – 1352 Ωm, and non-uniform spatial thickness distribution of about 1 m on the northwestern half to over 4 m at the southeastern end. This sequence's base lies the most resistive geo-electric layer, coded red/violet (>3015 Ωm). Lithologic inference of this sequence from top to bottom is loam, loamy sand, sand and dry sand respectively and it agrees with the lithological information of this area in Figure 3.

Profile 2 is a marked extension of profile 1 covering an additional 60 m (Figure 11). The imaged resistivity sequence of this subsurface section similarly exhibits identical recognizable order of layering with the first profile. Layering parameter range from the top to the base of the sequence are 74 Ωm – 126 Ωm and 0.9 m – 4 m depth, 135 Ωm – 418 Ωm and 2 m – 3 m deep, 500 Ωm – 1500 Ωm and 3 m – over 15 m depth, and >3000 Ωm with a depth of 60 m respectively; inferred in that corresponding order as loam, loamy sand, sand and dry sand.

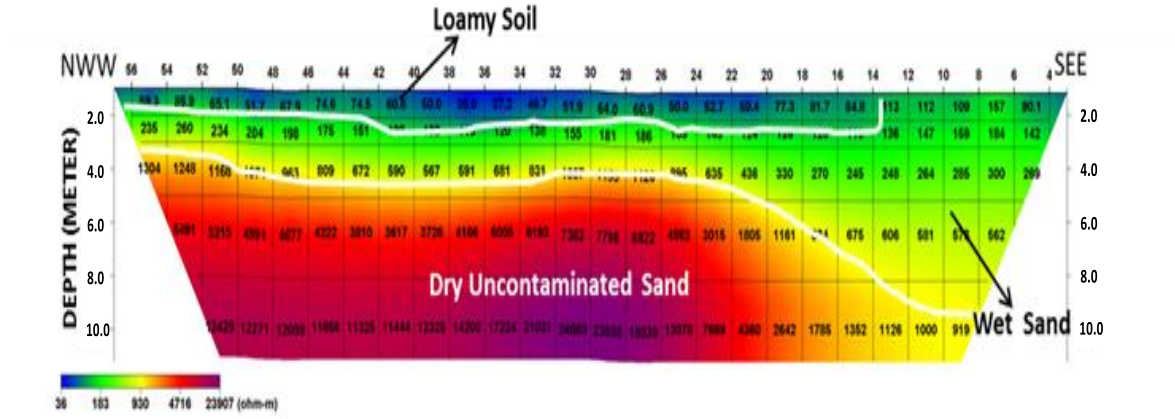

Figure 10-Interpreted resistivity model along with the first control profile

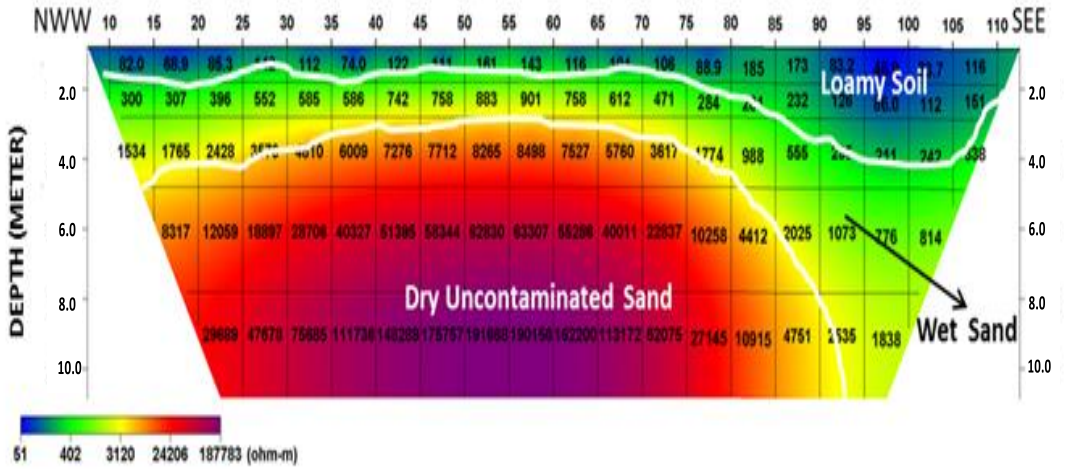

Figure 11-Resistivity model along the second control profile

Dumpsite Location 2 (Profile 3 and 4)

The resistivity image generated along with profile 3 (Figure 12) reveals anomalous zones of resistivity lows underlain by moderate to high resistivity zones. Contour range as delineated from top to the base of the subsurface section is 5 Ωm – 70 Ωm (blue-green – lemon coded contours), 100 Ωm – 206 Ωm (lemon coloured contours), 226 Ωm – 489 Ωm (yellow shaded contours), 521 Ωm – 2557 Ωm (reddish colouration) and >3000 Ωm (violet zone); essentially interpreted as leachate invaded contaminated zone, sandy clay, clayey sand, sand and dry sand. In the above respective order, thickness ranges between 2 m – over 10 m, 1 m – 2 m, 1 m – 2 m, 3 m – over 5 m, while that of the delineated basal layer extends to infinity.

Profile 4 is a marked extension of profile 3 with a further 60 m length increment (Figure 13). Along with this profile, there is a definite consistency of geo-electric layering as five resistivity strata were perceptibly depicted on its resistivity structure with values ranging from 5 Ωm – 83 Ωm (blue/green coded contours) inferred as leachate infiltrated zone, 101 Ωm – 190 Ωm (lemon) inferred as sandy clay, 205 Ωm – 474 Ωm (yellow) inferred as clayey sand, 529 Ωm – 1175 Ωm (red) inferred as sand and >2500 Ωm (violet) inferred as dry sand. The contamination zone's thickness range is within 3 m to 6 m, uniformly 1 m and 2 m thick for the sandy clay and clayey sand stratum, respectively. In comparison, the thickness of sand stratum ranges between 1 m – 5 m.

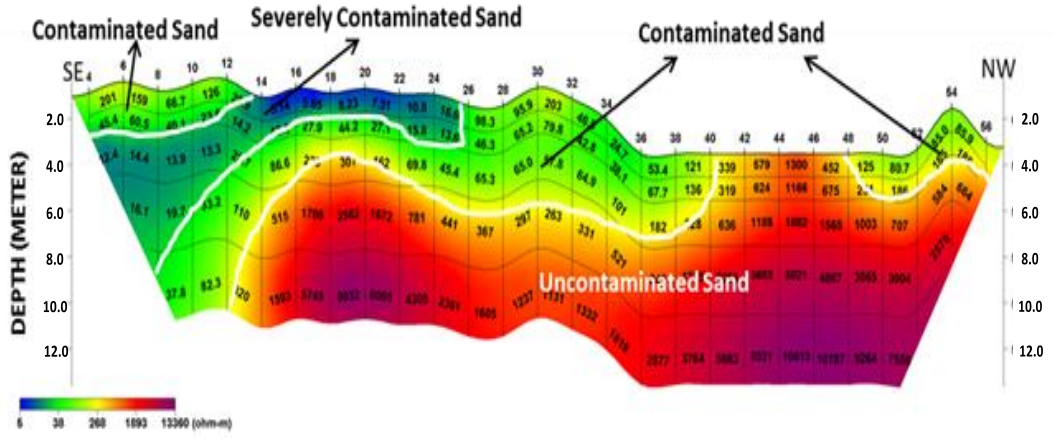

Figure 12- Resistivity model Structure along Profile 3

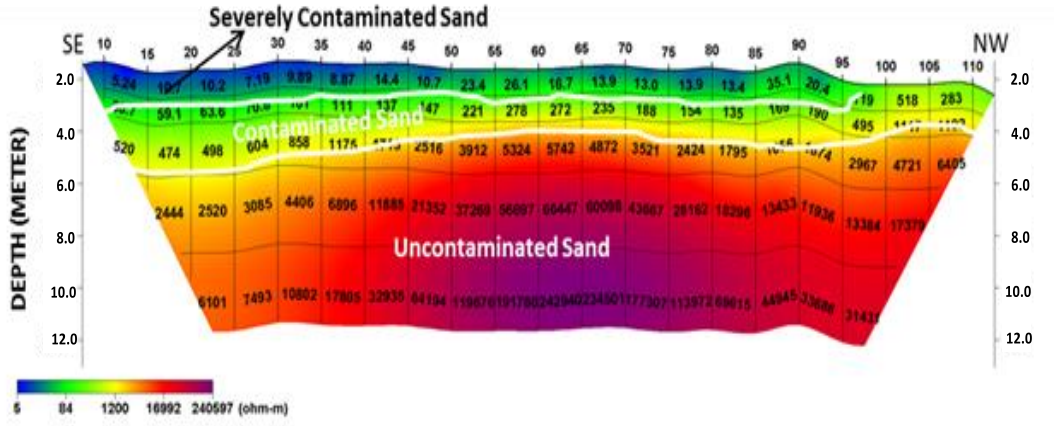

Figure 13- Resistivity model along Profile 4

Dumpsite Location 3 (Profile 5 and 6)

Resistivity autograph at location 3 is anomalously low in value when compared to the other two locations discussed above. Four (4) geo-electric units were delineated along with profile

5 (Figure 14). These units from the northwestern to southeastern end are characterized by an inherent resistivity range of 7 Ωm – 93 Ωm (blue/green), 100 Ωm – 173 Ωm (yellow), 206 Ωm – 418 Ωm (red) and 555 Ωm – 2347 Ωm (violet) corresponding to leachate invaded zone, sandy clay, clay sand and sand. The natural layering pattern observed at the control location appears entirely obscured by the high level of contamination occurring around this section of the dumpsite.

Furthermore, the extended profile (profile 6) at this location exposes the severity of penetration of the conductive contamination anomaly on the resistivity structure (Figure 15). From northwest to southeast, the resistivity value of each of the four delineated geo-electric units ranges between 10 Ωm – 91 Ωm (blue/green), 119 Ωm – 197 Ωm (yellow/brown), 222 Ωm – 418 Ωm (red) and 500 Ωm – 763 Ωm (violet); respectively inferred as contamination zone, sandy clay, clayey sand and sand.

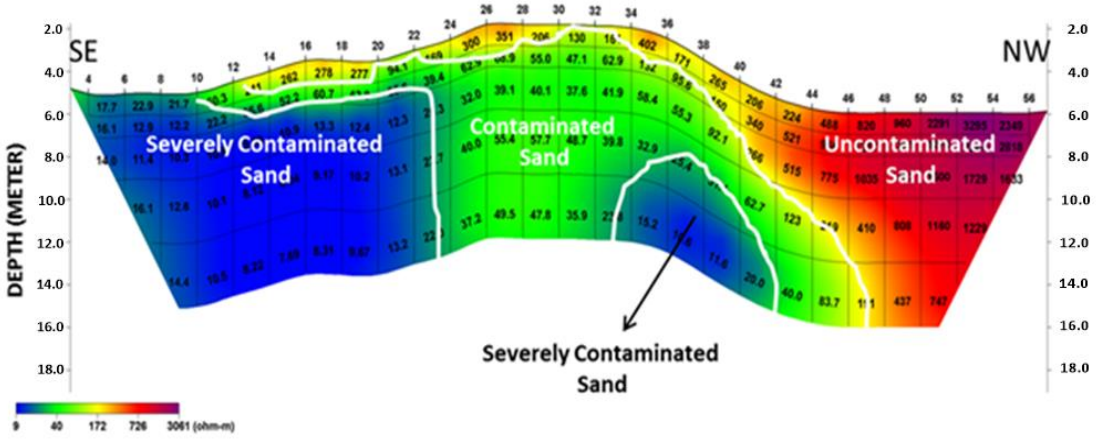

Figure 14-Interpreted Resistivity model along Profile 5

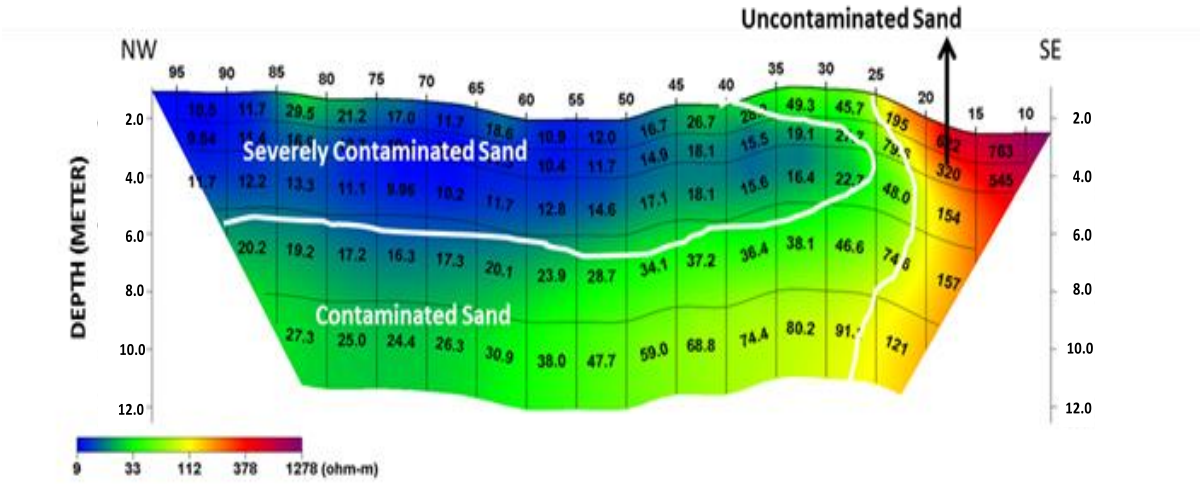

Figure 15- Interpreted Resistivity model along Profile 6

Protective Capacity

The best evaluative mechanism focuses on the protective capacity ratings at the control stations where no illusion of a very conductive stratum exists at the top of the sequence, as against the ambiguity created by the contaminated bed(s), which exhibits a 'pseudoclay-like' behaviour characterized by moderate longitudinal conductance. Therefore, the longitudinal conductance of the pollution-free zone is considered for the calculation of the protective capacity of the area as they serve as the control survey, i.e. VES 1, 2, 3 and 4 only. The longitudinal conductance of these four VES stations are 0.0048, 0.0151, 0.0057 and 0.0027,

respectively and this showed that the protective capacity of the area is poor as these values are lower than 0.10 (Table 2). This result, however agrees with the lithology and nature of the materials that made up the subsurface in this area, which is sandy, lacking the required earth filter to retard leachate substrate to infiltrate deeper down into the porous sand strata. The vulnerability of the subsurface aquifer to anthropogenic pollution is predictably high in the study area because of the porosity and permeability attributes of the Afowo sedimentsare, which is also high.

Lithological Log

In the studied section of the basin, sedimentary fills are almost entirely composed of continental sand facies. Lithologic logging of the area (Figure 15), in order of deposition; consists of basal conglomeratic sand, a thick pile of non-ferruginous sand, ferruginous sand and unconsolidated sand strata. The conglomeratic bed is sub-rounded in texture, lying unconformably on the partially weathered basement. Notable textural variation occurs within overlying sand strata, comprising medium to the coarse-grained aquiferous unit at the base but becomes finer at its upper part.

Correlating the electrical resistivity method, which is a remote approach and that of the obtained lithological log (in situ technique) shows significant correlation indicating the entire subsurface of the study location is mainly sand. Generally, the resistivity of uncontaminated sand is very high, but resistivity becomes low when it is saturated with leachate or fluid. Relating this to the study location, the area with a low resistivity value indicates the presence of contamination due to leachate infiltration. The resistivity of the control location in this research location shows a high resistivity value indicating the absence of leachate, while those within the dumpsite where contamination is noticeable shows a low resistivity value.

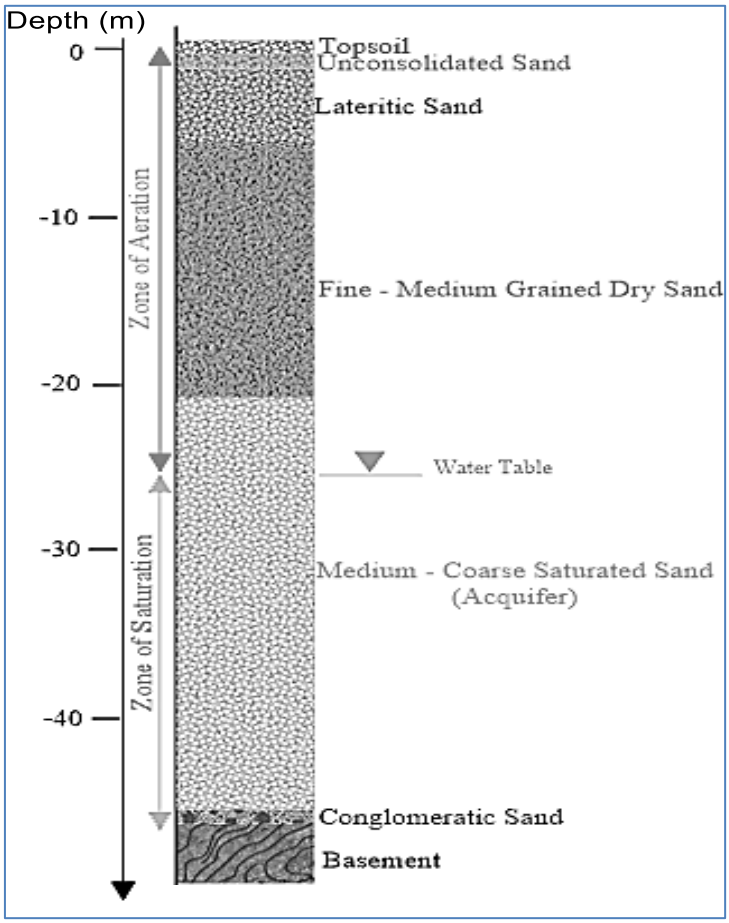

Figure 16- Lithostratigraphic Log of the Ijagun (within the study area). The water table was encountered at depth = 24m from the surface (elevation of point=189m)

Discussion

In the lithologic section information of the area, normal or horizontal stratification is the most evident sedimentary feature at the control area which corresponded with the resistivity structure that evidently revealed a mapped stratified sequence largely dominated by dry sand/sand strata overlain by thin layers of loam; averaging a thickness of 1m. These thin loamy caps cannot function effectively as subsurface protectors over the highly permeable sandy terrain, and thus would easily permit the invasion of harmful leachates into the underlying sandy beds.

Subsurface prevalence of leachates (both in terms of thickness and infiltration depth) and their spatial disposition are well delineated on the geoelectric sections and the interpreted dumpsite resistivity structures at the second and third locations. On a scale of severity using the rating of [15, 16 and 27], contamination level is far exceedingly acute at the southern and southeastern of the study area. Generally, adjacent to the highway, infiltrated depth hardly exceeds 10 m but farther away into the dumpsite, an alarming depth of leachate invasion greater than 25 m into the subsurface was mapped. From these observations, it can be emphatically elucidated that the natural environment has been greatly endangered by the down-flow and lateral encroachment of unwanted contaminants. More perturbing than the perceived superficial environmental decadence of the natural earth layers, and the pungent stinking atmospheric envelope is the possible acceleration of contaminants through the permeable sand strata into the groundwater of the area. Hence, drastic environmental control measures must be implemented to protect groundwater resources as the affected area, though within the vadoze zone has a prominent effect on its underlying aquifer.

Conclusion

Comparison of logging information, geo-electric sections and resistivity structures of the control area with those generated from the dumpsite confirm the environmental contamination of the underlying Afowo sand Formation beneath the dump. It can be concluded from the interpreted result that the produced electric section shows that the study area is underlined by topsoil, sand and dry sand. Resistivity values vary based on the level of contamination infiltration rate. High resistivity values indicated sand contamination-free regions while low resistivity values indicate leachate saturated region. The resistivity values increase with depth in most part of the survey area and this indicates that the infiltration rate of the leachate reduces with depth from the VES and 2D geoelectric section, Spatially, higher resistivity is observed in the control region of the study location while low value was observed within the dumpsite. The calculated longitudinal conductance also shows clearly that the protective capacity of the subsurface is Weak and this can best justify the easy migration of leachate in some parts of the study location and also correlate to the geology of the study area which is made up of mostly sand. The Perennial solution to this environmental problem is an outright relocation of the dumpsite to a better-protected location capped or underlain by thick clay stratum but in the absence of an alternative dumping ground, other sustainable strategies can be devised to manage the situation which includes the installation of waste recycling facilities on a dumpsite, conversion of municipal waste to methane gas for biomass energy generation, enforcement of stringent environmental rules and regulations, and periodical geophysical and geochemical assessment of pollution level of the study area.

Reference

[1] A. Rivera, *Canada's Groundwater Resources. Fitzhenry & Whiteside Limited, Markham*, Pp. 23-60, 2014.

[2] J.C. Agunwamba "Solid Waste Management in Nigeria: Problems and Issues" Environ. Manage. New York, vol. 22, no. 6, pp. 849-856, 1998.

[3] T. C. Ogwuelek "Municipal solid waste characteristics and management in Nigeria". *Iranian Journal of Environmental Health Science & Engineerin*g, vol. 6, no. 3, pp. 173-180, 2009.

[4] L.B. Osazua and N.K. Abdullahi "Geophysics Techniques for the Study of Groundwater Pollution, A Review". *Nigerian Journal of Physics*, vol. 20, no.1, pp. 163-174, 2008.

[5] N.K. Abdullahi, I.B. Osazuwa and P.O. Sule "Application of Integrated Geophysical Techniques in the Investigation of Groundwater Contamination: A Case Study of Municipal Solid Waste Leachate". *Ocean Journal of Applied Sciences*, vol. 4, pp. 7-25. ISSN 1943-2429, 2011.

[6] S Payal, "Deep trouble the hidden threat of groundwater pollution". *World Watch Paper*, pp. 55, 2000.ISBN: 1-878071-56-4

[7] N. J. George, A. I., Ubom and J. I. Ibanga "Integrated approach to investigate the effect of leachate on groundwater around the Ikot Ekpene dumpsite in Akwa Ibom State, Southeastern Nigeria", Hindawi publishing corporation *International Journal of Geophysics*, pp. 1-12, 2014, http://dx.doi.org/10.1155/2014/174589.(2013).

[8] K. Cartright and M.R. Mc Comas "Geophysical Surveys in Vicinity of Sanitary Landfill in Werth Eastern Illinois"; *Groundwater*, vol. 6, no. 5, pp. 23-30, 1968.

[9] W.B. Fink and D.B. Aulenhack, "Protracted Recharge of Treated Sewage into Sand, Part iv-Tracing the Flow of Contaminated" *Groundwater*, vol 12, no. 4, pp. 219-223, 1974.

[10] R.L. Stolar and P. Roux "Earth Resistivity Method for Determining Groundwater Contamination"; *Groundwater*, vol. 13, no. 2, pp. 145-150, 1975.

[11] J.P. Carpenter, R.S. Kanfman and B. Price "Use of Resistivity Sounding to Determine Landfill Structure"; *Groundwater*, vol. 28, pp. 569-575, 1990.

[12] R.D Barker "A Simple Algorithm for Electrical Imaging of the Subsurface". *First Break*, vol. 10, pp. 53-62, 1992.

[13] M.H. Loke, *Electrical Imaging Surveys for Environmental and Engineering Studies: A Practical Guide to 2-D and 3-D surveys. Geometrics, Sanjose, California*, USA, 1999.

[14] I. S. Mukhtar, P. Abdullatif, and M. Hanafi: "Detection of Groundwater Pollution using Resistivity Imaging at Seri Petang Landfill, Malaysia". *Journal of Environmental Hydrology*, vol. 8, pp. 1-8, 2000.

[15] R. S. Vivienne, *Hydrogeological, Geophysical and Hydrogeochemical Investigations of Groundwater Contamination by Leachate, Christchurch, New Zealand*, 1992.

[16] P.A. Enikanselu, "Detection and monitoring of –dumpsite-induced groundwater contamination using electrical resistivity method". *Pacific Journal of Science and Technology*, vol. 9, no 1: pp. 254-262, 2008.

[17] O. E. Agbasi, N. A. Aziz, Z. T. Abdulrazzaq, and S. E. Etuk, "Integrated Geophysical Data and GIS Technique to Forecast the Potential Groundwater Locations in Part of South Eastern Nigeria". *Iraqi Journal of Science*, 60(5), 1013-1022. (2019). Retrieved from https://ijs.uobaghdad.edu.iq/index.php/eijs/article/view/744

[18] E. U. Okpogo and P. E. Wilkie, "Delineation of leachate plume migration by electrical resistivity methods Ile Epo dumpsite, Lagos, Southwestern Nigeria". *Iraqi Journal of Science*, vol 59, no. 3, pp. 1614-1625, 2018. Retrieved from https://ijs.uobaghdad.edu.iq /index.php /eijs/article/view/452

[19] K.C. Burke, T.F.J. Dessauvagie and A.J Whiteman, "The Opening of the Gulf of Guinea and the Geological History of the Benue Depression and Niger Delta Native". *Physical Science*, vol. 223, pp. 51-55, 1971.

[20] M. E Omatsola and O. S. Adegoke, "Tectonic Evolution of Dahomey Basin". *Min. Geol*, vol. 54, pp. 65–87, 1981.

[21] O.K. Agagu, "A Geological Guide to Bituminous Sediments of Southwestern Nigeria", Unpublished Ph.D Thesis, Department of Geology, University of Ibadan, pp. 1-116,1985.

[22] H. Jones and R. D. Hockey, "The geology of part of south-western Nigeria: Geology Survey of Nigeria", *Bulletin*, vol. 31, pp. 87-100, 1964.

[23] HGebhardt, O. A. Adekeye and S. O Akande, "Late Paleocene to initial Eocene thermal maximum foraminifera biostratigraphy and paleoecology of the Dahomey Basin, southwestern Nigeria". *Gjahrbuch Der Geologischem Bundesantalt*, vol. 150, pp. 407–419, 2010.

[24] S.O. Olabode, and M.Z Mohammed, "Depositional Facies and Sequence Stratigraphic Study in Parts of Benin (Dahomey) Basin SW Nigeria: Implications on the Re-Interpretation of Tertiary

Sedimentary Successions", *International Journal of Geosciences*, vol. 7, pp. 210-228, 2016. http://dx.doi.org/10.4236/ijg.2016.72017.

[25] O. O. Bayewu, M. O. Oloruntola and G. O. Mosuro, "Assessment of Groundwater Prospect and Aquifer Protective Capacity using Resistivity Method in Olabisi Onabanjo University Campus, Ago-Iwoye, Southwestern Nigeria". *NRIAG Journal of Astronomy and Geophysics*, vol. 7, no. 2, pp. 347-360, 2018.

[26] T.E. Oni, G.O. Omosuyi and A.A. Akinlalu, "Groundwater vulnerability assessment using hydrogeologic and geoelectric layer susceptibility indexing at Igbara Oke, Southwestern Nigeria", *NRIAG Journal of Astronomy and Geophysics*, vol. 6, no. 2, pp. 452-458, 2017.

[27] A.O. Adelusi, "Aquifer mapping and assessment of its risk using electrical resistivity sounding technique in Akure metropolis, southwestern, Nigeria". *Nigeria Journal of Pure and Applied Physics*, vol. 4, pp. 65-73, 2009

[28] M.I. Oladapo, M.Z. Mohammed, O.O. Adeoye and B.A. Adetola, "Geoelectrical Investigation of the Ondo State Housing Corporation Estate Ijapo Akure, Southwestern Nigeria". *J. Mining Geol*., vol. 40, no. 1, pp. 41-48, 2004.